A plant/fungal-type phosphoenolpyruvate carboxykinase located in the parasite mitochondrion ensures glucose-independent survival of *Toxoplasma gondii*

Received for publication, June 19, 2017 Published, Papers in Press, July 18, 2017, DOI 10.1074/jbc.M117.802702

Richard Nitzsche[‡1], **Özlem Günay-Esiyok**[‡1,2], **Maximilian Tischer**[‡], **Vyacheslav Zagoriy**[§], **and Nishith Gupta**[‡3]

From the [‡]*Department of Molecular Parasitology, Humboldt University, 10115 Berlin, Germany and* [§]*metaSysX GmbH, 14476 Potsdam-Golm, Germany*

Edited by John M. Denu

Toxoplasma gondii **is considered to be one of the most successful intracellular pathogens, because it can reproduce in varied nutritional milieus, encountered in diverse host cell types of essentially any warm-blooded organism. Our earlier work demonstrated that the acute (tachyzoite) stage of *T. gondii* depends on cooperativity of glucose and glutamine catabolism to meet biosynthetic demands. Either of these two nutrients can sustain the parasite survival; however, what determines the metabolic plasticity has not yet been resolved. Here, we reveal two discrete phosphoenolpyruvate carboxykinase (PEPCK) enzymes in the parasite, one of which resides in the mitochondrion (*Tg*PEPCK$_{mt}$), whereas the other protein is not expressed in tachyzoites (*Tg*PEPCK$_{net}$). Parasites with an intact glycolysis can tolerate genetic deletions of *Tg*PEPCK$_{mt}$ as well as of *Tg*PEPCK$_{net}$, indicating their nonessential roles for tachyzoite survival. *Tg*PEPCK$_{net}$ can also be ablated in a glycolysis-deficient mutant, while *Tg*PEPCK$_{mt}$ is refractory to deletion. Consistent with this, the lytic cycle of a conditional mutant of *Tg*PEPCK$_{mt}$ in the glycolysis-impaired strain was aborted upon induced repression of the mitochondrial isoform, demonstrating its essential role for the glucose-independent survival of parasites. Isotope-resolved metabolomics of the conditional mutant revealed defective flux of glutamine-derived carbon into RNA-bound ribose sugar as well as metabolites associated with gluconeogenesis, entailing a critical nodal role of PEPCK$_{mt}$ in linking catabolism of glucose and glutamine with anabolic pathways. Our data also suggest a homeostatic function of *Tg*PEPCK$_{mt}$ in cohesive operation of glycolysis and the tricarboxylic acid cycle in a normal glucose-replete milieu. Conversely, we found that the otherwise integrative enzyme pyruvate carboxylase (*Tg*PyC) is dispensable not only in glycolysis-competent but also in glycolysis-deficient tachyzoites despite a mitochondrial localization. Last but not least, the observed physiology of *T. gondii* tachyzoites appears to phenocopy cancer cells, which holds promise for developing common therapeutics against both threats.**

Toxoplasma gondii is an obligate intracellular parasite of the protozoan phylum Apicomplexa, which is capable of infecting and replicating in most vertebrate organisms, including humans. The disease acute toxoplasmosis is hallmarked by tissue necrosis as a consequence of incessant host cell lysis following rapid intracellular proliferation of the tachyzoite stage (1). Previous work has demonstrated that glucose and glutamine are the two major carbon sources utilized during the lytic cycle of tachyzoites (2–4). Glucose is imported through a high-affinity glucose transporter (GT1)[4] located in the plasma membrane of the parasite (2). It is subsequently catabolized to pyruvate by glycolytic enzymes located in the cytosol (5, 6), a major fraction of which is converted into lactate (3). A second pool of pyruvate enters the mitochondrion and is used to produce acetyl-CoA, which condenses with oxaloacetate to produce citrate to drive the TCA cycle (7). Oxaloacetate can be generated from glucose-derived pyruvate and/or from glutamine catabolism through the TCA cycle (3).

One of the principal metabolic phenotypes observed in fast multiplying cells is an induction of aerobic glycolysis (*i.e.* the Warburg effect), which is distinguished by increased glucose catabolism and lactate synthesis (8). Besides glucose, glutamine is another major nutrient utilized as an anaplerotic substrate for the TCA cycle in proliferating cells (9). Glycolysis and TCA cycle together not only produce energy and reducing equivalents for cellular functioning, but also deliver carbon for the biogenesis of nucleotides, lipids, amino acids, and intermediates of one-carbon metabolism (8). Likewise, whereas glucose is an important contributor to the cellular energy and carbon

This work was supported by German Research Foundation Grants GU1100/3-1 and GU1100/4-1 and Heisenberg Fellowship GU1100/8-1 (to N. G.). Financial support to R. N. was provided through grants awarded to N. G. The authors declare that they have no conflicts of interest with the contents of this article.

This article contains supplemental Table S1 and Figs. S1–S5.

The nucleotide sequence(s) reported in this paper has been submitted to the GenBank™/EBI Data Bank with accession number(s) KX785383, KX785384, and KX785385

[1] Both authors contributed equally to this work.

[2] Recipient of an Elsa Neumann fellowship.

[3] To whom correspondence should be addressed: Dept. of Molecular Parasitology, Humboldt University, Philippstrasse 13, House 14, 10115 Berlin, Germany. Tel.: 49-30-20936404; Fax: 49-30-20936051; E-mail: Gupta.Nishith@staff.hu-berlin.de.

[4] The abbreviations used are: GT1, glucose transporter 1; IT, insertional tagging; COS, crossover sequence; ATc, anhydrotetracycline; HFF, human foreskin fibroblast; PEP, phosphoenolpyruvate; Pyr, pyruvate; 3PG, 3-phosphoglyceraldehyde; G3P, glycerol 3-phosphate; G6P, glucose 6-phosphate; R5P, ribose 5-phosphate; 2OG, 2-oxoglutarate; Suc, succinate; Fum, fumarate; Mal, malate; Cit, citrate; UPRT, uracil phosphoribosyltransferase; TCA, tricarboxylic acid; PyC, pyruvate carboxylase; PEPCK, phosphoenolpyruvate carboxykinase; FBP, fructose-1,6-bisphosphatase; FUdR, 5-fluorodeoxyuridine; DHFR-TS, dihydrofolate reductase thymidylate synthase; MOI, multiplicity of infection; UPLC, ultraperformance liquid chromatography.

pools in tachyzoites, glutamine is another central carbon source, which feeds into the TCA cycle and contributes to the bioenergetic requirements (3, 4). Interestingly, tachyzoites are quite resilient to genetic and biochemical perturbations of carbon metabolism (2, 4). In particular, they can survive the genetic deletion of the major glucose transporter, GT1. The Δ*tggt1* mutant displays an impaired glycolysis accompanied by a compensatory increase in glutamine catabolism and activation of otherwise negligible gluconeogenesis. The mechanism by which glycolysis-deficient tachyzoites ensure their glucose-independent survival and reproduction in human host cells remains enigmatic, however.

In mammalian tissues, pyruvate can be converted back to glucose by gluconeogenesis when glucose supply becomes limited (10). The latter route is not a simple reversal of glycolysis; it involves additional reactions catalyzed by pyruvate carboxylase (PyC), phosphoenolpyruvate carboxykinase (PEPCK), fructose-1,6-bisphosphatase (FBP) and glucose-6-phosphatase. In the first step, pyruvate is carboxylated by PyC to produce oxaloacetate that is simultaneously decarboxylated and phosphorylated by PEPCK to yield phosphoenolpyruvate (PEP) in a GTP-dependent manner (10). PEP undergoes sequential catalysis by a series of glycolytic enzymes to produce fructose 1,6-bisphosphate, which is eventually hydrolyzed to fructose 6-phosphate by FBP enzyme. At last, glucose-6-phosphatase hydrolyzes glucose 6-phosphate (G6P), formed by isomeric conversion of fructose 6-phosphate, to produce glucose. PyC and PEPCK also function as typical anaplerotic and cataplerotic enzyme, respectively, ensuring a continual operation of TCA cycle during rapid biosynthetic activities. In tumor cells, glucose-dependent PyC-mediated anaplerosis allows cells to grow in the absence of glutamine (11). Conversely, cytosolic and mitochondrial isoforms of PEPCK (PEPCK-C/M) are required to support the growth of cancer cells from glutamine under glucose-starved conditions (12, 13).

The *T. gondii* genome harbors all gluconeogenic enzymes except for glucose 6-phosphatase (14). We have already characterized two isoforms of FBP in *T. gondii*, *Tg*FBP1 and *Tg*FBP2, only the latter of which is involved in gluconeogenesis (15). *Tg*FBP2 has another critical function (*i.e.* futile cycling), which makes the FBP activity essential even in tachyzoites with functional glycolysis. It has thus not been possible to test the significance of glutamine-derived carbon and gluconeogenesis in parasites with a defective glycolysis. In this work, we generated a set of mutants in glycolysis-competent and glycolysis-deficient backgrounds and discovered the mitochondrial PEPCK as a key regulator of metabolic plasticity in *T. gondii*. *Tg*PEPCK$_{mt}$ mediates a metabolic shunt to counterbalance glycolytic defect, which furnishes carbon from glutamine to satisfy the bioenergetic demands of tachyzoites. Our results ascertain PEPCK$_{mt}$-dependent metabolic reprogramming as a major mechanism by which tachyzoites manage in a low-glucose environment.

Results

Pyruvate carboxylase is a mitochondrial protein but it is not expressed in tachyzoites

PyC is a member of the biotin-dependent enzyme family. It catalyzes physiologically irreversible carboxylation of pyruvate to yield oxaloacetate in a broad range of prokaryotes and eukaryotes (16). Our bioinformatics search using the yeast and mammalian isoforms identified one putative PyC in the genome database of *T. gondii* (TGGT1_284190; www.ToxoDB.org).[5] We cloned the complete ORF of *Tg*PyC, which encodes for a protein of 1391 amino acids with a conserved catalytic domain. Ectopic overexpression of C-terminally tagged *Tg*PyC (*Tg*PyC-HA) in intracellular tachyzoites revealed that the protein is localized in the mitochondrion, as confirmed by immunofluorescent staining with a known organelle marker, *Tg*F1B-ATPase (17) (Fig. 1*A*). Subsequently, we epitope-tagged the corresponding gene to gauge its native expression (Fig. 1*B*). Unexpectedly, neither by immunofluorescence nor by immunoblot assays were we able to detect the *Tg*PyC-HA protein in parasites (Fig. 1, *C* and *D*).

To corroborate the absence of *Tg*PyC expression under normal glucose-replete conditions, we utilized anti-biotin antibody staining the prosthetic group (Fig. 1*E*). Yet again, we failed to detect immunostaining of the parasite mitochondrion. In contrast, we were able to detect another biotin-dependent enzyme, acetyl-CoA carboxylase (18) that localized with ferredoxin, a marker of the apicoplast in tachyzoites (19). Next, we tested the endogenous expression of *Tg*PyC in the Δ*tggt1* strain to investigate whether PyC protein is produced under a glycolysis-deficient environment (Fig. 1*E*). Contrary to our notion, we did not see a detectable induction of *Tg*PyC in the Δ*tggt1* strain either. Taken together, several conclusions can be drawn from these unforeseen data sets. First, PyC is a mitochondrial protein, whose gene is transcribed but the transcript is not translated, which indicates its post-transcriptional regulation in parasites. An apparent lack of PyC expression implies its negligible contribution in proliferating (biosynthetically active) parasites with functional glycolysis. Equally, metabolic importance of pyruvate carboxylase in the absence of sugar transport can also be relegated.

Pyruvate carboxylase is dispensable for the lytic cycle of tachyzoites

In proliferating mammalian cells, one of the established functions of PyC is to drive anaplerosis under normal conditions (16). A second equally important function is to power gluconeogenesis under glucose starvation. To investigate the anaplerotic as well as the gluconeogenic significance of *Tg*PyC in parasites, we engineered the knock-out mutants in glycolysis-competent and glycolysis-deficient strains, respectively. The *TgPyC* gene was deleted by homologous recombination-mediated insertion of the dihydrofolate reductase thymidylate synthase (DHFR-TS) expression cassette (supplemental Fig. S1*A*). The absence of *Tg*PyC transcript in representative clones of the Δ*tgpyc* and Δ*tggt1*/Δ*tgpyc* strains confirmed the genetic ablation of pyruvate carboxylase (supplemental Fig. S1*B*). The successful making of the two mutants shows that *Tg*PyC is not required for the survival of tachyzoites. The mutants were assessed for the overall growth fitness in plaque assays (supplemental Fig. S1*C*). None of the knock-out strains of *Tg*PyC

[5] Please note that the JBC is not responsible for the long-term archiving and maintenance of this site or any other third party hosted site.

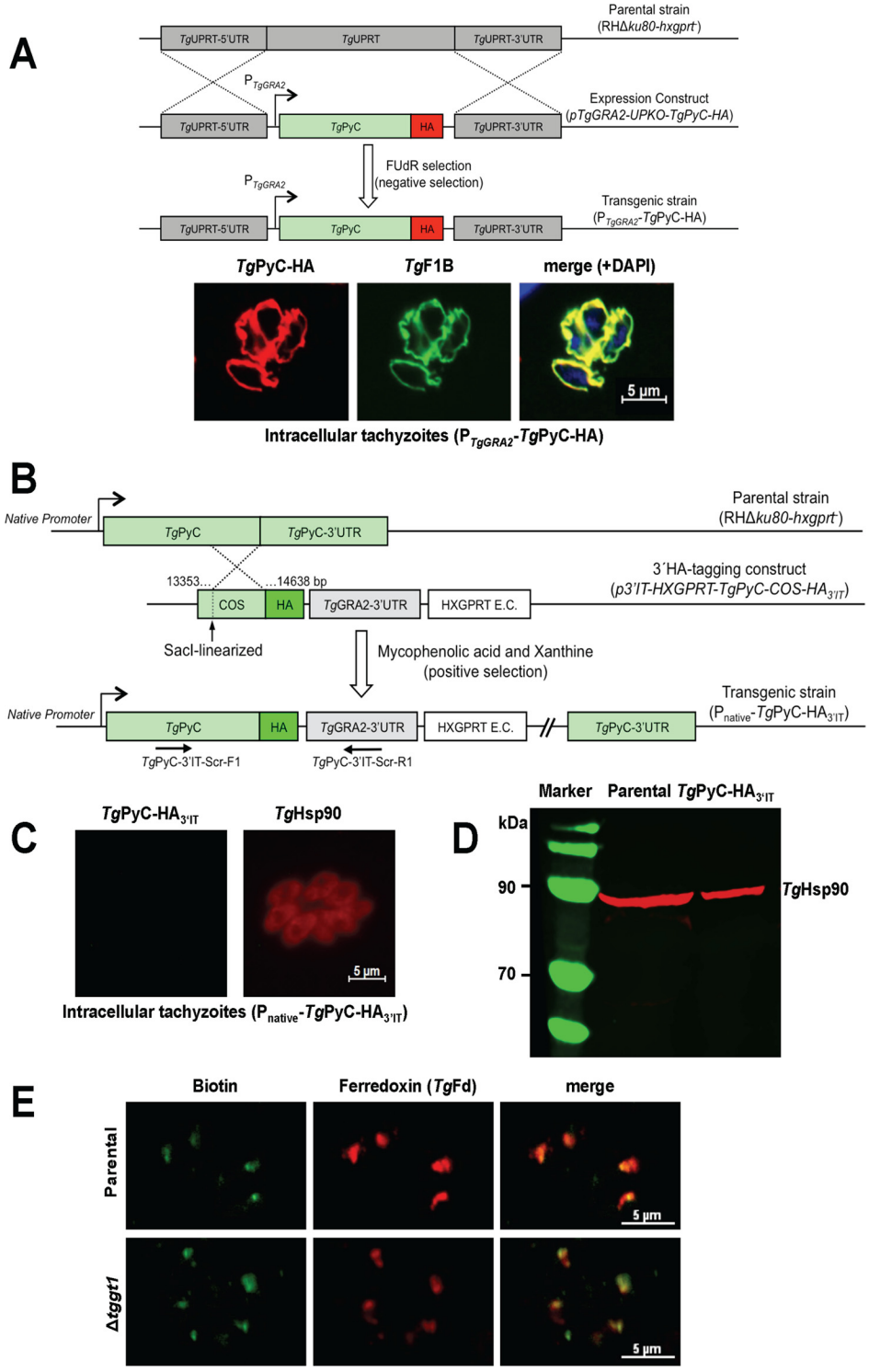

Figure 1. Ectopically overexpressed pyruvate carboxylase resides in the parasite mitochondrion; however, its endogenous expression is not detectable in the tachyzoite stage of *T. gondii*. *A*, schematics of the expression strategy and immunofluorescence images showing subcellular distribution of PyC in tachyzoites. A single copy of *Tg*PyC tagged with HA and regulated by the *TgGRA2* elements was targeted at the *TgUPRT* locus via double homologous recombination in the RHΔ*ku80-hxgprt*$^-$ strain. Stable transgenic parasites were selected by FUdR for the loss of UPRT function and subjected to immunostaining with α-HA and α-*Tg*F1B antibodies. DAPI staining shows the parasite and host cell nuclei. *B*, genomic tagging of the endogenous *Tg*PyC with a C-terminal HA epitope in tachyzoites. The construct for 3′-insertional tagging of the *TgPyC* gene contained a COS and HXGPRT expression cassette (*E.C.*). It was linearized by SacI enzyme and transfected in the RHΔ*ku80-hxgprt*$^-$ strain. Parasites expressing *Tg*PyC-HA$_{3'IT}$ under the control of native promoter and *TgGRA2* 3′-UTR were drug-selected and screened by genomic PCR using recombination-specific primers (*Tg*PyC-3′IT-Scr-F1/R1) and sequencing of the transcript. *C* and *D*, detection of *Tg*PyC-HA$_{3'IT}$ by immunofluorescence and Western blot analysis. Intracellular parasites (24-h infection) were immunostained with α-HA and α-*Tg*Hsp90 antibodies to monitor the endogenous expression and location of *Tg*PyC-HA$_{3'IT}$. For immunoblot, extracellular tachyzoites (10^7) were subjected to SDS-PAGE, blotting, and staining with α-HA and α-*Tg*Hsp90 (loading control) antibodies. *E*, detection of *Tg*PyC in the parental (RHΔ*ku80-hxgprt*$^-$) and Δ*tggt1* strains using α-biotin and α-*Tg*Fd antibodies. Note that only acetyl-CoA carboxylase co-localizing with ferredoxin in the apicoplast is visible, which confirms immunodetection of the biotin prosthetic group.

exhibited a noteworthy defect. The size as well as the number of plaques formed by the Δ*tgpyc* and Δ*tggt1*/Δ*tgpyc* mutants were comparable with respective progenitor strains. These results resonate with insignificant expression of pyruvate carboxylase in the tachyzoite stage (Fig. 1, *C–E*) and establish its physiological dispensability during the lytic cycle irrespective of glucose import.

The genome of T. gondii harbors two distinctive orthologs of PEPCK

A surprisingly nonessential nature of *Tg*PyC prompted us to examine the metabolic relevance of PEPCK for the asexual reproduction of tachyzoites in glucose-replete and glucose-deprived states. We identified two PEPCK paralogs, *Tg*PEPCK1 (TGGT1_289650) and *Tg*PEPCK2 (TGGT1_289930) in the parasite database (www.ToxoDB.org)[5] encoding for 677 and 614 amino acids, respectively (supplemental Fig. S2). Sequence alignment with *bona fide* orthologs confirmed the presence of a complete catalytic domain containing substrate-, metal-, and nucleotide-binding residues (supplemental Fig. S2*A*). MitoProt analysis predicted >95% probability of *Tg*PEPCK1 being targeted to the mitochondrion via a mitochondrial targeting peptide (supplemental Fig. S2*B*). Phylogenetic clustering demonstrated that *Tg*PEPCK1 forms a distinct clade with other PEPCKs from the phylum apicomplexa and closely related to the ATP-dependent orthologs from fungi and plants (supplemental Fig. S2*C*). *Tg*PEPCK2 is markedly distinct from *Tg*PEPCK1 and shows substitutions of otherwise-conserved residues in the nucleotide- and substrate-binding sites. Quite notably, orthologs of *Tg*PEPCK2 appear to be absent in most organisms; they could only be identified in selected coccidian parasites (*e.g. Neospora caninum*, *Hammondia hammondi*).

Subsequently, we determined the endogenous expression and subcellular localization of the two PEPCK isoforms in tachyzoites. To this end, we performed crossover-mediated tagging of both genes with a 3′-HA epitope (Fig. 2, *A* and *B*). Immunofluorescence staining established that C-terminally HA-tagged *Tg*PEPCK1 (*Tg*PEPCK1-$HA_{3'IT}$) was distributed in the mitochondrion, which was confirmed by its costaining with the organelle marker *Tg*F1B-ATPase (17) (Fig. 2*A*). By contrast, *Tg*PEPCK2-$HA_{3'IT}$ was not detectable in tachyzoites despite a successful epitope-tagging of its gene (Fig. 2*B*). Consistently, we were able to amplify transcript of *Tg*PEPCK1 but not of *Tg*PEPCK2, further corroborating the expression of only former isoform (see Fig. 3*C* and supplemental Fig. S3*B*). Immunoblot analysis confirmed the constitutive expression of *Tg*PEPCK1-$HA_{3'IT}$ (~76 kDa), whereas *Tg*PEPCK2-$HA_{3'IT}$ was not detectable (Fig. 2*C*). Following these data, we renamed *Tg*PEPCK1 as *Tg*$PEPCK_{mt}$ (mitochondrial) and *Tg*PEPCK2 as *Tg*$PEPCK_{net}$ (not expressed in tachyzoites). According to transcriptomics data (20), *Tg*$PEPCK_{net}$ is significantly induced during development of the parasite in the felid host (enteroepithelial stages; Fig. 2*D*). Hence, it appears as if *Tg*$PEPCK_{mt}$ and *Tg*$PEPCK_{net}$ serve different developmental stages in the asexual and sexual hosts, respectively, during the natural lifecycle of *T. gondii*.

TgPEPCK$_{mt}$ is required for an optimal lytic cycle under glucose-replete conditions

We examined the biological importance of both PEPCKs in the glycolysis-competent as well as in glycolysis-deficient mutants. First, we generated the mutants of *Tg*$PEPCK_{net}$ in the standard (RHΔ*ku80*-TaTi) and its derivative Δ*tggt1* strains by exchanging the gene with a DHFR-TS selection cassette via double homologous recombination (supplemental Fig. S3*A*). In agreement with the aforementioned results (Fig. 2*C*), neither the parental nor the Δ*tggt1* strain displayed the expression of *Tg*$PEPCK_{net}$ transcript (supplemental Fig. S3*B*). Consequently, the resulting Δ*tgpepck*$_{net}$ and Δ*tggt1*/Δ*tgpepck*$_{net}$ mutants also lacked the mRNA of *Tg*$PEPCK_{net}$. No significant impairment in the plaque area or plaque number of the single and double mutants was evident when compared with the respective progenitor strains (supplemental Fig. S3*C*). It can therefore be concluded that *Tg*$PEPCK_{net}$ is not required during the lytic cycle of tachyzoites.

Using a similar approach, we examined the physiological requirement of *Tg*$PEPCK_{mt}$ for the parasite in the presence or absence of glucose transport (Fig. 3*A*). Indeed, we were able to knock out the *TgPEPCK$_{mt}$* locus by introducing a DHFR-TS expression cassette, albeit only in the standard parental (RHΔ*ku80*-TaTi) strain. Pyrimethamine-resistant parasite clones were screened by genomic PCR, which displayed amplification of 5′ and 3′ recombination-specific bands in selected clones (Fig. 3*B*). Sequencing of amplicons from a clone representing the Δ*tgpepck*$_{mt}$ mutant confirmed the deletion of the *TgPEPCK$_{mt}$* locus. As expected, the Δ*tgpepck*$_{mt}$ mutant lacked the transcript expression, further endorsing the gene knock-out (Fig. 3*C*). The mutant formed smaller plaques (30% growth defect) when compared with the parental strain, whereas plaque numbers were not changed (Fig. 3*D*). To ascertain the requirement of *Tg*$PEPCK_{mt}$ in glucose-limiting conditions, we attempted to delete the gene in the Δ*tggt1* strain. However, our multiple efforts to make a Δ*tggt1*/Δ*tgpepck*$_{mt}$ mutant were futile. These data show that mitochondrial PEPCK is required for efficient growth in glucose-replete conditions but nonessential for parasite survival. It becomes refractory to knock-out upon glycolytic defect, denoting a vital role of the enzyme under glucose-deprived conditions.

TgPEPCK$_{mt}$ is critical for glucose-independent growth of tachyzoites

An apparent lethality of the Δ*tggt1*/Δ*tgpepck*$_{mt}$ mutant prompted us to engineer an inducible knockdown of *Tg*$PEPCK_{mt}$ in the Δ*tggt1* strain (Δ*tggt1*/iΔ*tgpepck*$_{mt}$). To achieve this, we first introduced an anhydrotetracycline (ATc)-regulated and C-terminally HA-tagged ORF of *Tg*$PEPCK_{mt}$ at the uracil phosphoribosyltransferase (*TgUPRT*) locus by 5-fluorodeoxyuridine (FUdR) selection and subsequently ablated the gene by DHFR-TS selection cassette (Fig. 4*A*). As envisaged, *Tg*$PEPCK_{mt}$ transcript was significantly repressed (not detectable) upon treatment of the mutant with ATc for 72 h (Fig. 4*B*). Consistently, immunofluorescence and immunoblot assays endorsed a marked inhibition of the protein in the

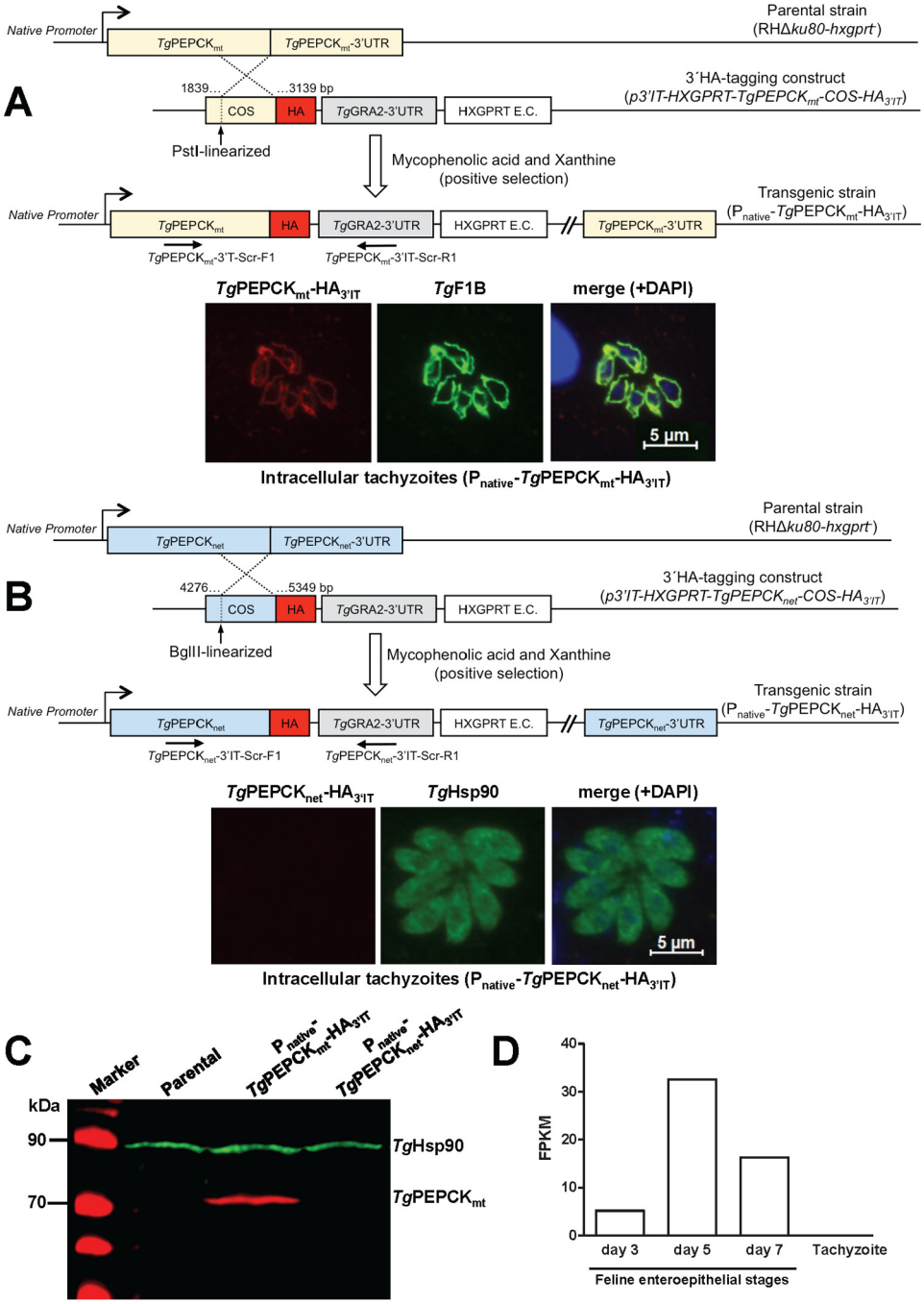

Figure 2. *Tg*PEPCK$_{mt}$ (*Tg*PEPCK1) localizes in the mitochondrion, whereas *Tg*PEPCK$_{net}$ (*Tg*PEPCK2) is not expressed in the tachyzoite stage of *T. gondii*. *A*, 3′-insertional tagging of the *TgPEPCK$_{mt}$* gene with a HA tag in tachyzoites and detection of *Tg*PEPCK$_{mt}$-HA$_{3'IT}$ protein by immunofluorescence. The PstI-digested plasmid construct with a COS targeting the 3′-end of the *TgPEPCK$_{mt}$* gene was transfected into the RHΔ*ku80-hxgprt*$^-$ strain. Tachyzoites encoding *Tg*PEPCK$_{mt}$-HA$_{3'IT}$ under the control of its native promoter and *TgGRA2* 3′-UTR were selected with the indicated drugs, screened by genomic PCR using *Tg*PEPCK$_{mt}$-3′IT-Scr-F1/R1 primers, and verified by sequencing. Intracellular parasites (24-h infection) were immunostained with α-HA and α-*Tg*F1B antibodies to determine the subcellular location of *Tg*PEPCK$_{mt}$-HA$_{3'IT}$ and treated with DAPI to visualize the cell nuclei. *B*, genomic tagging of the *TgPEPCK$_{net}$* gene and fluorescent detection of *Tg*PEPCK$_{net}$-HA$_{3'IT}$ in tachyzoites. Stable transgenic parasites were generated and immunostained with α-HA and α-*Tg*Hsp90 antibodies, as stated in *A*. *C*, immunoblotting showing the natural expression of *Tg*PEPCK$_{mt}$-HA$_{3'IT}$, *Tg*PEPCK$_{net}$-HA$_{3'IT}$, and *Tg*Hsp90 in transgenic tachyzoites from *A* and *B*. Extracellular parasites (10^7) of the indicated strains were subjected to protein isolation followed by SDS-PAGE and immunostaining using α-HA and α-*Tg*Hsp90 (loading control) antibodies. Parental strain served as a negative control for α-HA staining. *D*, comparative levels of *Tg*PEPCK$_{net}$ RNA in the tachyzoite and merozoite stages of *T. gondii*. The graph is reproduced from the parasite database (www.ToxoDB.org)[5] based on previous work of A. B. Hehl *et al.* (20). Tachyzoites were grown *in vitro*; merozoites were isolated from enterocytes of the cyst-infected cats on specified days. The *y* axis denotes transcript levels of fragments per kilobase of exon model per million mapped reads (*FPKM*), as measured by standard paired-end Illumina sequencing of the parasite mRNA.

Δ*tggt1*/iΔ*tgpepck$_{mt}$* strain within a day of ATc treatment, which was not detectable upon prolonged exposure to the drug (see 48–72 h in Fig. 4, *C* and *D*). A chemically repressible conditional mutant of *Tg*PEPCK$_{mt}$ in the Δ*tggt1* strain enabled us to evaluate its importance for glucose-independent plaque growth of tachyzoites (Fig. 5, *A* and *B*). As expected, the precursor Δ*tggt1* mutant was not impacted by treatment with ATc, whereas the double mutant was severely impaired upon

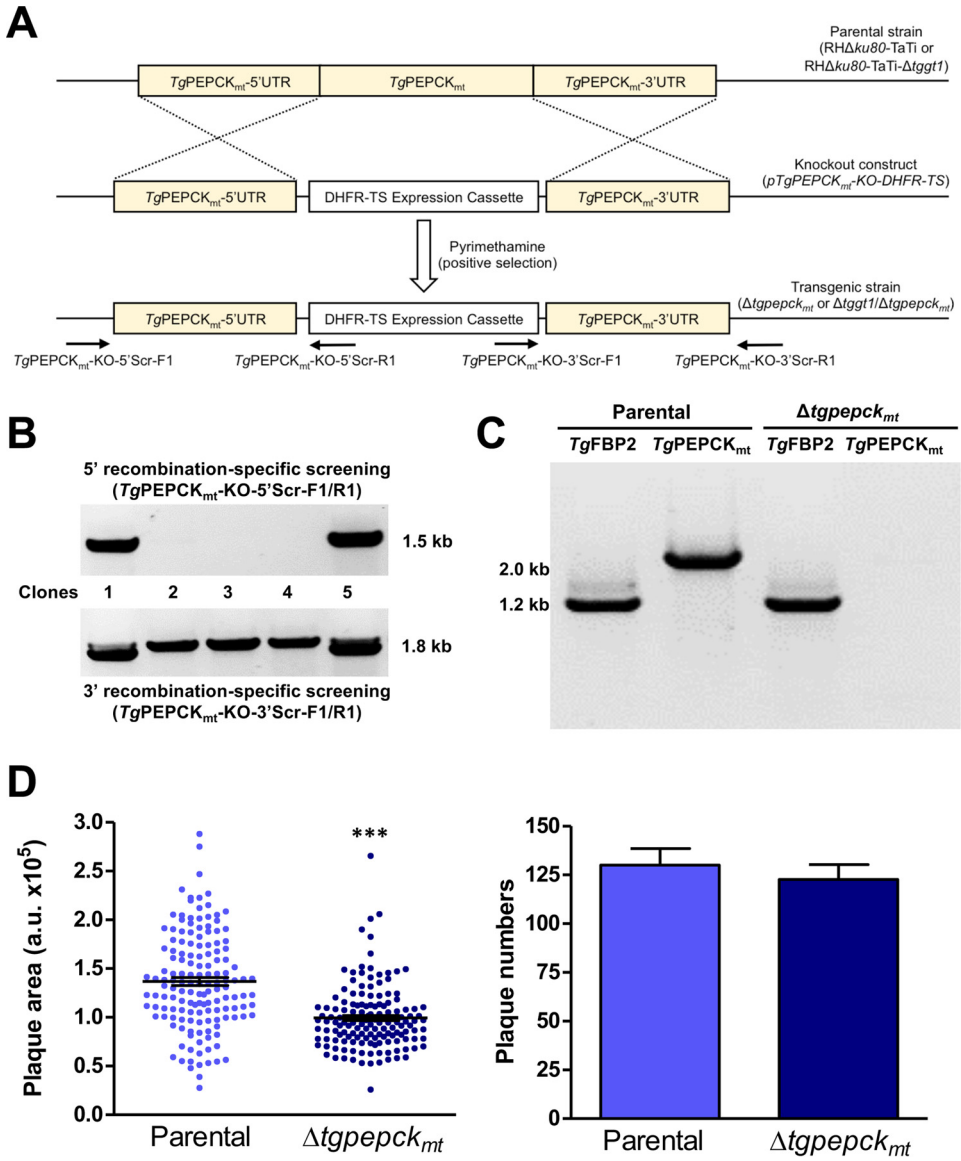

Figure 3. *Tg*PEPCK$_{mt}$ promotes the lytic cycle of glycolysis-competent tachyzoites. *A*, scheme depicting double homologous recombination-mediated knock-out of the *TgPEPCK$_{mt}$* gene by DHFR-TS in tachyzoites. The construct was transfected into the indicated parental strains, and pyrimethamine-resistant clonal parasites were screened for 5′- and 3′-crossover events using applicable primer pairs (*Tg*PEPCK$_{mt}$-KO-5′Scr-F1/R1 or *Tg*PEPCK$_{mt}$-KO-3′Scr-F1/R1). *B*, genomic PCR screening showing 5′ and 3′ recombination in selected parasite clones generated according to the scheme described in *A*. The specificity of the *TgPEPCK$_{mt}$* knock-out in recombination-positive clones was confirmed by sequencing of PCR amplicons. *C*, validation of the Δ*tgpepck$_{mt}$* mutant by transcript analysis. A representative clonal mutant was examined for the presence or absence of *Tg*PEPCK$_{mt}$ and *Tg*FBP2 (control) transcripts using ORF-specific primer sets. Parental strain was included as a positive control. *D*, plaque assays revealing comparative growth of the Δ*tgpepck$_{mt}$* mutant with respect to its parental strain. Shown are the area (arbitrary units) and number of plaques (mean ± S.E. (*error bars*), $n = 3$ assays). Significance was tested using Student's *t* test (***, $p < 0.001$).

repression of *Tg*PEPCK$_{mt}$. The conditional mutant formed miniscule-size plaques, although their numbers were comparable with the Δ*tggt1* strain. Our measurements of growth rates by serial passage (Fig. 5*C*) demonstrated a continued unaltered reproduction of the Δ*tggt1* mutant irrespective of ATc. Likewise, the double mutant behaved normally without ATc but slowed progressively during successive passages and eventually ceased to grow upon drug exposure. The assay showed a continued but increasingly slowing growth until day 7 (168 h), although the protein was undetectable by Western blotting within 48 h of the drug treatment (Fig. 4*D*). The observed yield pattern probably reflects a steadily declining residual activity of *Tg*PEPCK$_{mt}$ in parasites. Taken together, these results demonstrate an essential role of the mitochondrial PEPCK in glycolysis-deficient tachyzoites.

TgPEPCK$_{mt}$ regulates glutamine-derived gluconeogenic flux in tachyzoites

To discern the underlying basis of observed phenotype in the Δ*tggt1*/iΔ*tgpepck$_{mt}$* mutant, we performed stable isotope labeling assays. The mutant was cultured with or without ATc for 60–72 h and then labeled in standard medium (with or without ATc), in which glutamine was exchanged by [U-^{13}C]glutamine. The viability of the parasite inoculum was >95% for both conditions. Label inclusion analysis of the central metabolites using GC-MS showed a notable flux of glutamine-derived carbon into metabolites associated with TCA cycle and gluconeogen-

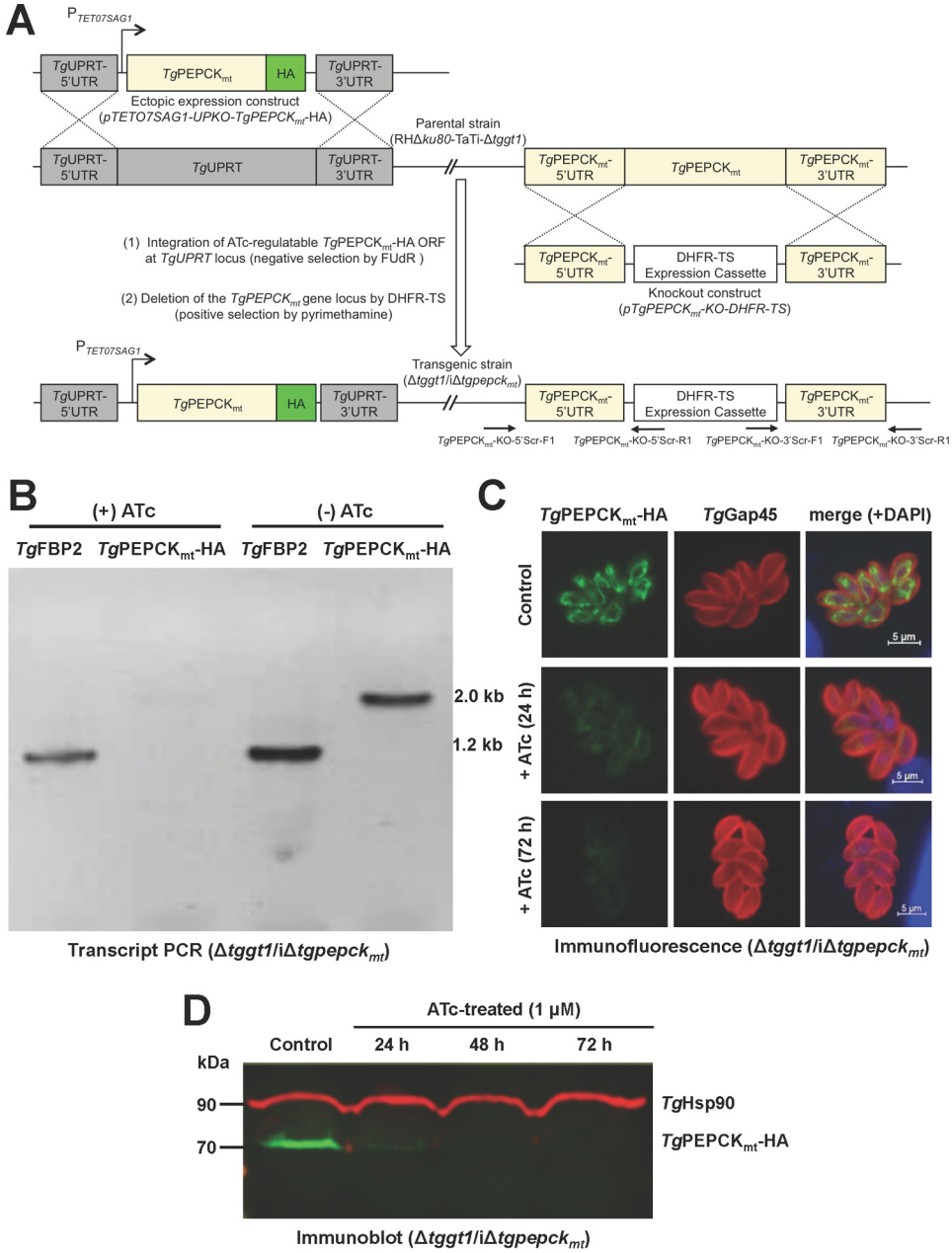

Figure 4. Conditional mutagenesis enables a tetracycline-regulated knockdown of *Tg*PEPCK$_{mt}$ in glycolysis-impaired tachyzoites. *A*, scheme for generating a tetracycline-inducible mutant of *Tg*PEPCK$_{mt}$ (iΔ*tgpepck$_{mt}$*) in a GT1 knock-out strain with impaired glycolysis (RHΔ*ku80*-TaTi-Δ*tggt1*). In the first step, an ATc-repressible ORF of *Tg*PEPCK$_{mt}$-HA was integrated at the *TgUPRT* locus by FUdR selection, and then the *TgPEPCK$_{mt}$* gene was replaced by DHFR-TS. The eventual Δ*tggt1*/iΔ*tgpepck$_{mt}$* mutant was identified by genomic PCR using 5′ and 3′-crossover-specific primers (*Tg*PEPCK$_{mt}$-KO-5′Scr-F1/R1 and *Tg*PEPCK$_{mt}$-KO-3′Scr-F1/R1). *B*, PCR confirming the regulation of *Tg*PEPCK$_{mt}$ transcript by ATc in the Δ*tggt1*/iΔ*tgpepck$_{mt}$* mutant. Total parasite RNA was used to amplify *Tg*PEPCK$_{mt}$-HA and *Tg*FBP2 (control for RNA integrity) using ORF-specific primers. *C*, immunostaining of the Δ*tggt1*/iΔ*tgpepck$_{mt}$* strain showing ATc regulation of *Tg*PEPCK$_{mt}$-HA protein. The untreated control and drug-treated parasites were stained using α-HA and α-*Tg*Gap45 (a marker of inner membrane complex) antibodies. *D*, immunoblot depicting the ATc-mediated repression of *Tg*PEPCK$_{mt}$-HA in the conditional mutant. Parasites (10^7) were subjected to immunoblot analyses using α-HA and *Tg*Hsp90 (loading control) antibodies.

esis in the on-state, as judged by comparing the abundance of non-labeled compounds with the summed intensities of all of their detected isotopomers (Fig. 6). ATc treatment resulted in reduced inclusion of ^{13}C from glutamine into select metabolites linked to gluconeogenesis (PEP, 3PG, G3P, R5P, and Pyr) that was reflected in their abundance (supplemental Fig. S4*A*). We also observed somewhat modest but evident decrease in labeling of certain TCA cycle intermediates (Cit, 2OG, Suc, Fum, Mal), although the abundance of these metabolites did not mirror the isotope inclusion (supplemental Fig. S4*B*), probably due to anaplerosis of other substrates, which seems not to be the case for gluconeogenesis. A combined assessment of all glutamine-labeled metabolites confirmed a perturbed gluconeogenesis and TCA cycle when expression of *Tg*PEPCK$_{mt}$ was turned off (Fig. 7). Impairment of gluconeogenesis was more obvious than impairment of the TCA cycle.

Interestingly, all six possible isotopomers of citrate were detected, suggesting the occurrence of a whole TCA cycle

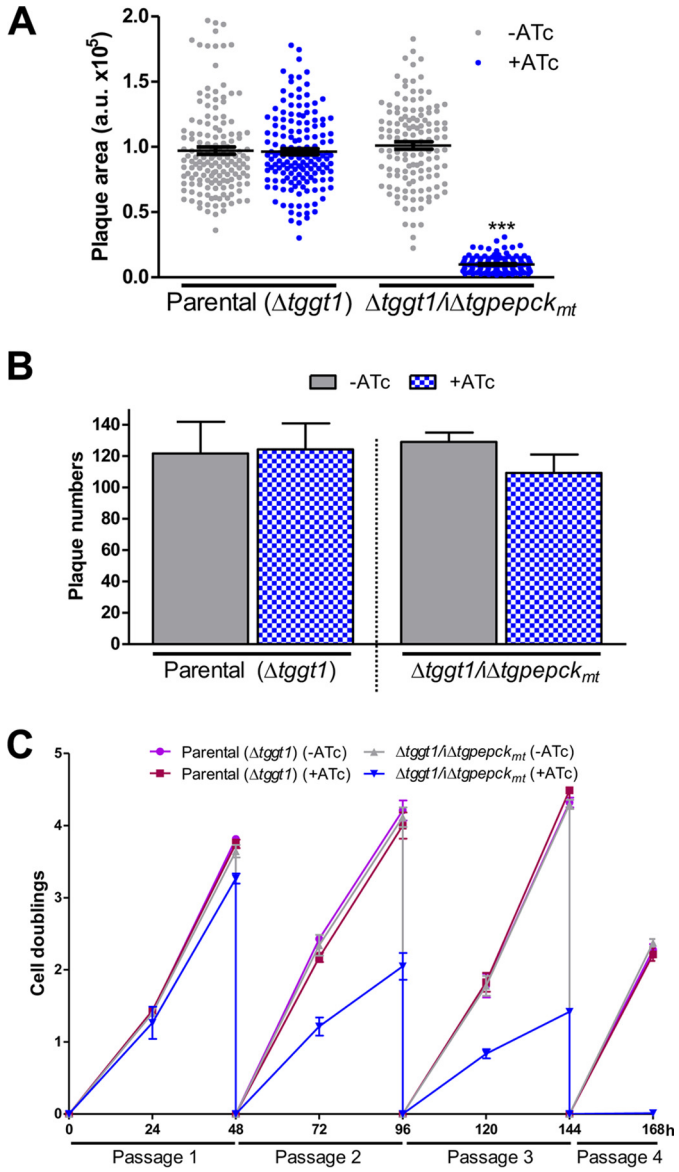

Figure 5. *Tg*PEPCK$_{mt}$ is essential for the lytic cycle of tachyzoites with impaired glycolysis. *A* and *B*, growth phenotype of the ATc-regulatable Δ*tggt1*/iΔ*tgpepck*$_{mt}$ strain with respect to the parental tachyzoites. The *Tg*PEPCK$_{mt}$ mutant and parental (RHΔ*ku80*-TaTi-Δ*tggt1*) strains were evaluated by plaque area (arbitrary units) and numbers in the absence or presence of ATc. Statistical analysis was done by Student's *t* test (***, $p < 0.001$; mean ± S.E. (*error bars*), $n = 3$ assays). *C*, cell doublings of the indicated strains over a period of four serial passages. Tachyzoites cultured with or without ATc (MOI = 1) were syringe-released from host cells to calculate the yield and determine the replication rates ($n = 3$ assays).

fueled by glutamine only. The M+6 citrate isotopomer is derived from M+5 citrate after its cleavage by an ATP citrate lyase to produce M+2 acetyl-CoA. The latter is condensed with M+4 oxaloacetate to form M+6 citrate. The M+4 oxaloacetate comes from M+5 α-ketoglutarate via succinyl-CoA, succinate, fumarate, and malate. Likewise, the occurrence of M+5 citrate indicates that the citric acid cycle steps between α-ketoglutarate and citrate are reversible via backward functioning of isocitrate dehydrogenase, as reported previously in mammalian cells (21, 22). These findings underline *Tg*PEPCK$_{mt}$ as a metabolic shunt connecting the mitochondrial and cytosolic flux of glutamine-derived carbon and entail the presence of reductive carboxylation in *T. gondii* tachyzoites.

A knockdown of TgPEPCK$_{mt}$ impairs the ribose biosynthesis in the Δtggt1/iΔtgpepck$_{mt}$ mutant

Due to reversible nature of many reactions of the TCA cycle and glycolysis/gluconeogenesis as well as existence of multiple "branching points" in these pathways, the carbon flux cannot be quantitatively estimated on the basis of isotopic labeling of central metabolites presented above. Hence, to obtain additional proof of the carbon transfer from glutamine to metabolites of gluconeogenesis, we determined the incorporation of glutamine-derived carbon into the ribose moiety of RNA that can only occur via gluconeogenesis and subsequent pentose phosphate pathway. Our previous work has demonstrated the incorporation of [^{14}C]glutamine into RNA of the GT1 mutant, suggesting glutamine's role in biomass production via gluconeogenesis (4). Here, we inspected the inclusion of [U-^{13}C]glutamine into RNA nucleosides to demonstrate that *Tg*PEPCK$_{mt}$ plays a crucial role in biogenesis of macromolecules under glycolytic deficiency.

The Δ*tggt1*/iΔ*tgpepck*$_{mt}$ mutant was labeled with [^{13}C]glutamine during its intracellular growth, followed by extraction and hydrolysis of the parasite RNA. Ultraperformance liquid chromatography (UPLC)-MS analysis of hydrolyzed sample revealed labeling of adenosine, guanosine, and uridine (Fig. 8*A*). Uridine showed an ~80% inclusion of glutamine-derived carbon in the *Tg*PEPCK$_{mt}$ mutant, whereas adenosine and guanosine were only modestly (~20%) labeled. A lower rate of label inclusion in purines as compared with uridine is consistent with the fact that tachyzoites are auxotrophic for purines (relying on the host cell), whereas they are competent in synthesizing pyrimidines (23, 24).

To discriminate whether the nucleoside labeling is primarily due to incorporation of glutamine carbon into the ribose moiety or into the base, we performed UPLC-MS/MS analysis of all of the isotopomers of uridine and guanosine. We estimated the intensities of the unlabeled as well as of the labeled ribose fragments (Fig. 8*B*), which confirmed a significant inclusion of ^{13}C in uridine-bound ribose, but not in guanosine-bound sugar. Chemical repression of *Tg*PEPCK$_{mt}$ by ATc treatment resulted in a significant decrease of label incorporation into uridine-ribose. We recorded a decline across the individual isotopomers except for I+3 upon treatment with ATc (Fig. 8*C*). In brief, these results indicate that the pentose phosphate shunt is impaired upon knockdown of the mitochondrial PEPCK, endorsing a function of PEPCK$_{mt}$ in macromolecular synthesis via the gluconeogenic pathway.

Discussion

Our work suggests that *Tg*PEPCK$_{mt}$ serves as a nodal enzyme, which coordinates glycolysis, gluconeogenesis, and TCA cycle under glucose-rich conditions to support anabolic activities in tachyzoites (Fig. 9). In sugar-starved cells, *Tg*PEPCK$_{mt}$ enables the production of glutamine-derived biosynthetic precursors and ensures a canonical TCA cycle. Consistent with the absence of the glucose-6-phosphatase gene, tachyzoites do not produce glucose from [^{13}C]glutamine,

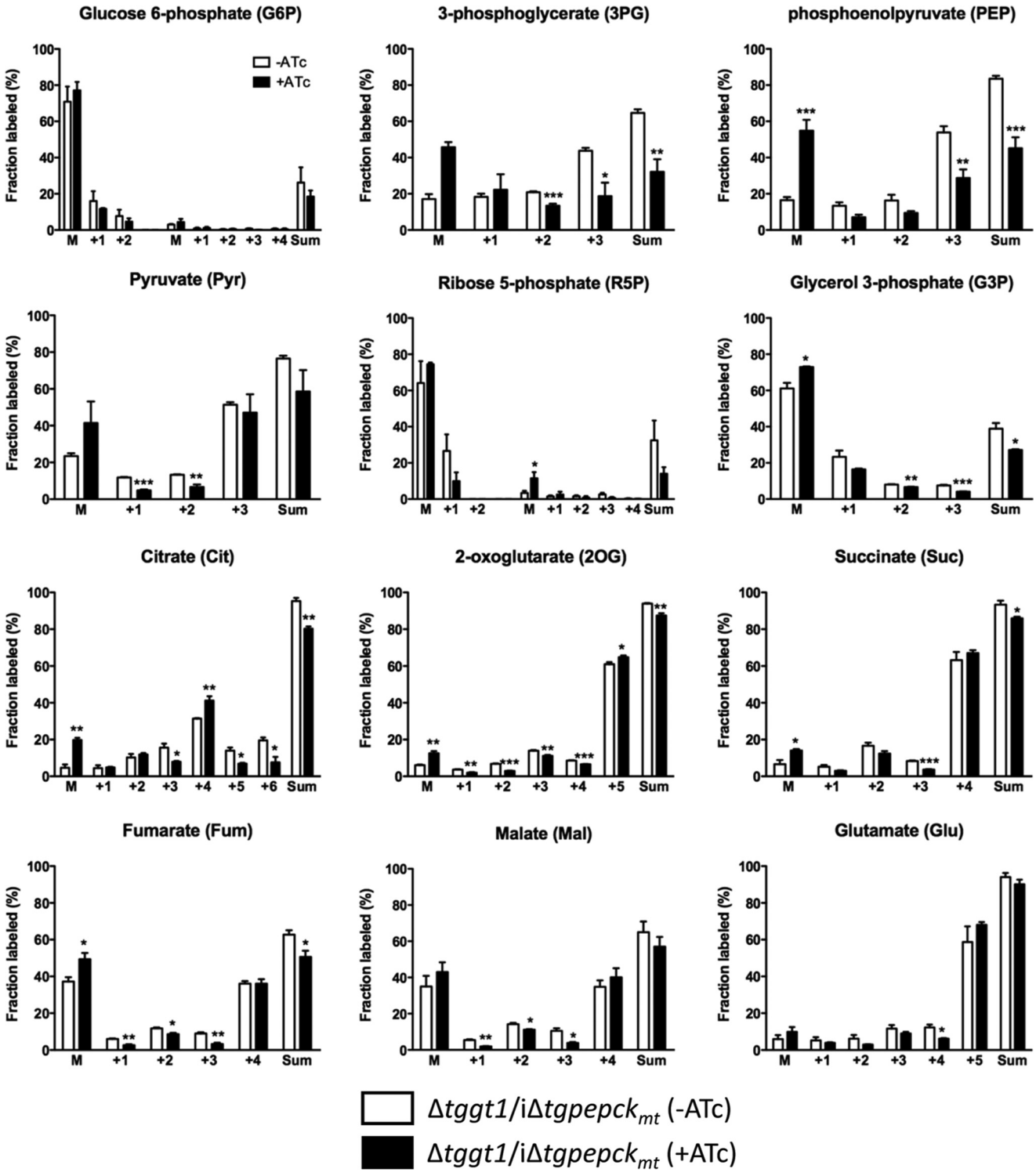

Figure 6. Fractional abundance of the select isotopomers in the Δ*tggt1*/i*Δtgpepck*$_{mt}$ tachyzoites labeled with [U-^{13}C]glutamine. Isotope inclusion was evaluated by metabolic labeling of intracellular tachyzoites with [U-^{13}C]glutamine (4 h, 37 °C, 5% CO_2). Polar metabolites were isolated from isotope-labeled parasites and subjected to GC-MS analysis. *M*, unlabeled fraction; *Sum*, collective abundance of all ^{13}C-containing isotopomers of a given metabolite. Only fragmented analytes were detectable for G6P and R5P. Note that our experimental design of metabolomics had to make a reasonable trade-off between obtaining a sufficient amount of purified tachyzoites for the metabolite measurements and maximum growth inhibition (a proxy for the enzyme activity). This trade-off was best met between days 3 and 4 of ATc treatment, on which the parasite growth is still nearly the half-maximum (see Fig. 5*C*). The obvious explanation for the residual labeling in the off-state mutant is that knockdown of PEPCK$_{mt}$ is incomplete in the conditions used to prepare samples for metabolomic analysis. In particular, when we inferred enzymatic activity from reduction in PEP labeling (a direct product of PEPCK$_{mt}$), we observed a decline of ~50%, which is consistent with the growth (half-maximum) at the time of sample collection. Statistical significance was determined separately for each group (with or without ATc) using Student's *t* test ($n = 4$ assays; *, $p < 0.05$; **, $p < 0.01$; ***, $p < 0.001$). *Error bars*, S.E.

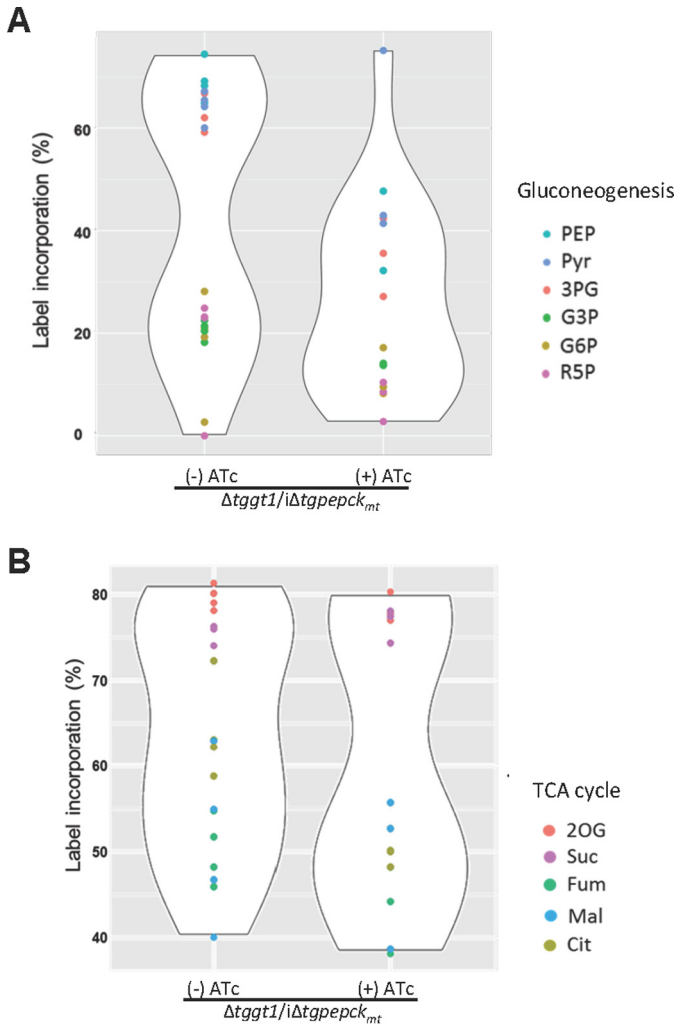

Figure 7. *Tg*PEPCK$_{mt}$ regulates the flux of glutamine-carbon through gluconeogenesis and TCA cycle. *A* and *B*, violin plots showing the impairment of glutamine flux into metabolites involved in or directly associated with gluconeogenesis and TCA cycle in the Δ*tggt1*/iΔ*tgpepck*$_{mt}$ mutant. Intracellular parasites were labeled as described in Fig. 6 (see "Materials and methods" for additional details). Fractional abundance of ^{13}C in selected metabolites is depicted ($n = 4$ assays). The extent of variation in the contour of ATc-treated samples is proportional to the degree of perturbation in aggregate carbon flux via a given pathway.

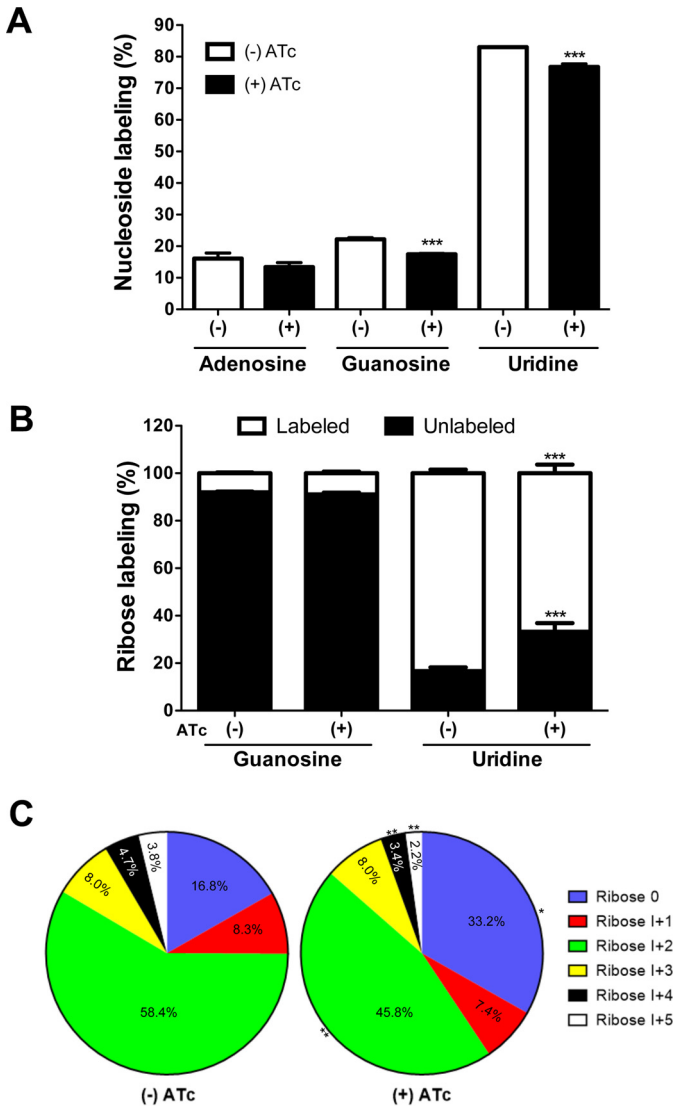

Figure 8. Glutamine-derived carbon is utilized for synthesis of RNA in the Δ*tggt1*/iΔ*tgpepck*$_{mt}$ strain. *A*, inclusion of ^{13}C in adenosine, guanosine, and uridine nucleosides of RNA labeled with [U-^{13}C]glutamine (12 h, 37 °C, 5% CO_2) in the presence or absence of ATc. The figure shows general labeling based on the total ion current data, which do not discriminate between the label in ribose or base. *B*, stable isotope labeling of ribose in nucleosides, as deduced by MS/MS. The labeling of ribose in adenosine was undetectable, and in guanosine, it was >10%. The minor labeling of purines appears to be a consequence of isotope inclusion in the base, probably through glycine and CO_2 derived from glutamine's usage through the TCA cycle. *C*, fractional abundance of the ^{13}C atoms in all isotopomers of the ribose moiety of uridine. Percentage fractions of the unlabeled (*Ribose 0*) and labeled isotopomers (*I+1* to *I+5*) are displayed for the drug-treated and control samples. Statistical analysis was done using Student's *t* test (*, $p < 0.05$; **, $p < 0.01$; ***, $p < 0.001$; mean ± S.E. (*error bars*), $n = 4$ assays).

which signifies that the parasite engages in all steps of gluconeogenesis except for dephosphorylation of G6P and fully consumes gluconeogenic intermediates to drive biosynthetic activities required for glucose-independent survival. Glutamine anaplerosis can more or less totally recompense for glucose anaplerosis and maintains the operation of the TCA cycle as a source for energy and a biosynthetic hub. The function of the citric acid cycle is guaranteed at least in part via the synthesis of glutamine-derived pyruvate, which can be converted to acetyl-CoA for oxidation in the mitochondrion in a manner similar to glucose-deprived cancer cells (12, 13). Even in glucose-replete conditions, given the choice between glucose and glutamine-dependent anaplerosis, the latter should be favored because PyC is not expressed in tachyzoites. Also from an energetic perspective, PyC uses one ATP per oxaloacetate molecule (16), whereas glutaminolysis does not need ATP; instead, glutamine catabolism yields reducing equivalents for oxidative phosphorylation and enzymatic reactions (25).

Although a continued operation of the TCA cycle and oxidative phosphorylation by glutamine may produce adequate energy and reductive power to drive invasion and sustain enzymatic catalysis, it cannot entirely account for the replication of glucose-starved tachyzoites because glycolytic metabolites are still needed to generate the macromolecules essential for the cell proliferation. For instance, glutamine-derived 3PG, G3P, and R5P serve as precursors for the synthesis of amino acids, glycerophospholipids, and nucleotides, respectively, in cancer cells (25). Our previous study (4) has shown that glucose-

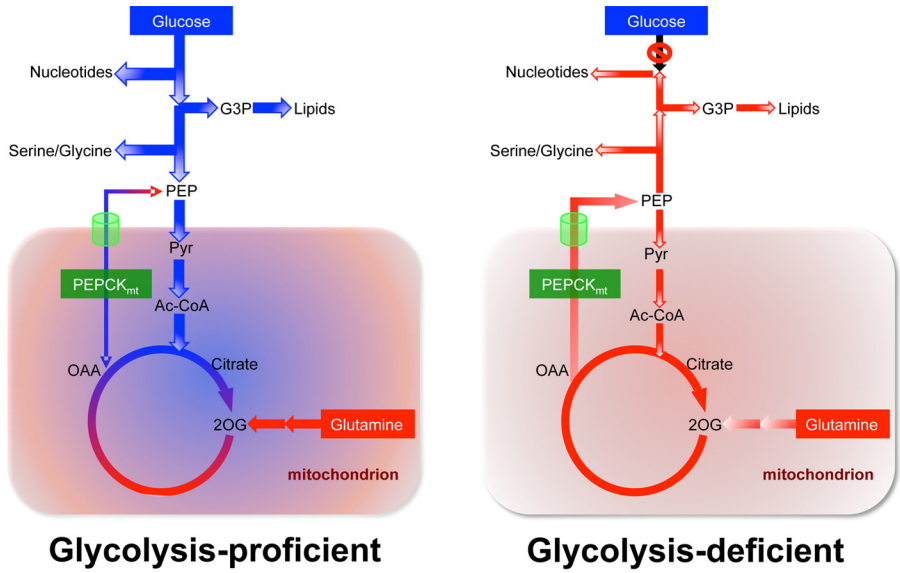

Figure 9. A prototype model featuring the function of *Tg*PEPCK$_{mt}$ as a metabolic shunt in central carbon metabolism of tachyzoites. Schemes are constructed based on this study and earlier work. In cells with an intact glycolysis (*left*), the mitochondrial PEPCK maintains a homeostatic bidirectional flow of glucose and glutamine-derived carbon, which may enable integrated use of both nutrients and rapid metabolic rewiring in response to nutritional oscillations within and/or outside host cells. Neither glucose nor glutamine alone produces significant amounts of fully labeled citrate, suggesting co-usage of both nutrients to operate the TCA cycle (depicted by *green/red colors*). A minor amount of (+6)-citrate that is produced from glucose requires a pool of sugar-derived oxaloacetate probably generated by *Tg*PEPCK$_{mt}$, because *Tg*PyC and *Tg*PEPCK$_{net}$ are not expressed and expendable during the lytic cycle. On the other hand, in glycolysis-impaired cells (*right*), *Tg*PEPCK$_{mt}$ allows glutamine-fueled gluconeogenic flux to ensure the biosynthetic activities and thereby parasite survival. Likewise, *Tg*PEPCK$_{mt}$-derived PEP and ensuing recycling of pyruvate can sustain a glutamine-fueled TCA cycle that is critical to produce energy and reducing equivalents. The work also implicates the presence of a PEP transporter in the membrane of the mitochondrion.

derived carbon is incorporated into protein, glycerophospholipids, and nucleotides. Indeed, inclusion of glutamine-derived carbon into 3PG, G3P, and R5P is up-regulated in the absence of glucose import (4) and declined upon repression of *Tg*PEPCK$_{mt}$ (this study), indicating a vital role of glutamine in biomass synthesis following glycolytic deficiency (Fig. 9). Such a decrease in the level of macromolecule precursors upon repression of PEPCK$_{mt}$ impairs the biomass production and leads to eventual demise of the conditional mutant. It is also worth noting here that two carbon atoms in nitrogenous bases originate from glycine, and two one-carbon units are derived from N^{10}-formyl-tetrahydrofolate, which requires serine (25). Synthesis of both serine and glycine demands 3PG, initially made from glutamine in the Δ*tggt1* strain. Accordingly, the addition of excess serine and glycine can bypass the knockdown of *Tg*PEPCK$_{mt}$ in the Δ*tggt1*/iΔ*tgpepck*$_{mt}$ mutant, as judged by a partial rescue of the phenotype (supplemental Fig. S5). The fact that the lytic cycle was not restored entirely is consistent with additional bioenergetic routes served by glutamine that could not be satisfied by other nutrients present in the parasite culture.

In mammalian and yeast cells, other noncarbohydrate precursors of gluconeogenesis include pyruvate, lactate, glycerol, fatty acids, and selected amino acids. It will now be interesting to investigate whether glutamine can supply biosynthetic precursors adequately enough to support the parasite survival or whether ancillary nutrients also play a significant role. None of the specified nutrients rescued the severe growth defect in the Δ*tggt1*/iΔ*tgpepck*$_{mt}$ strain (not shown). The Δ*tggt1* mutant is unable to utilize exogenous pyruvate, and lactate synthesis depends on the extent of glucose catabolism (2–4). Glycerol may enter gluconeogenesis at dihydroxyacetone phosphate, but consistent with its inability to restore the plaque growth, the enzyme glycerol kinase could not be found in the parasite genome. β-Oxidation of fatty acids may provide yet another source for biosynthetic growth under glucose limitation (26), although there is no genetic or biochemical evidence of this pathway in *T. gondii*. Other anaplerotic nutrients capable of making oxaloacetate may include branched-chain amino acids (leucine, valine, isoleucine), which can enter the TCA cycle through metabolism of propionyl-CoA. The metabolic relevance of this pathway in tachyzoites is not clear, however (27). Taken together, these data underpin the importance of glutaminolysis over alternative routes during the lytic cycle, which is further intensified by the fact that glutamine is the second most abundant nutrient in the parasite culture and in human blood plasma after glucose (28).

A role of PEPCK in promoting the entry of carbon from glutamine into biosynthetic precursors via PEP converges with cancer cells. Montal *et al.* (12) and Vincent *et al.* (13) found that certain tumor cells reprogram selected metabolic pathways to meet their increased biosynthetic needs, particularly when glucose levels are low in their microenvironment. They observed that activities of PEPCK-C and PEPCK-M are required to produce intermediates of nucleic acid from glutamine in a glucose-limited environment. PEP fuels the pentose phosphate shunt and serine/glycine metabolism, both of which contribute to the synthesis of nucleotides required for cell proliferation. Utilization of glutamine and anabolic diversion of intermediates therefore appears to be a common strategy exploited by proliferating tachyzoites and tumor cells to counteract a dearth of glucose. PEPCK-M mRNA and protein are induced upon withdrawal of glucose in tumor cells (29). The catalytic activity of PEPCK enzymes also depends on GTP (30) and acetylation–deacetylation (31). Surprisingly, *Tg*PEPCK$_{mt}$ is constitutively

expressed and appears to be ATP-dependent, which suggests a singular regulation of gluconeogenesis by an acetylation–deacetylation mechanism in *T. gondii*. Indeed, acetylation of *Tg*PEPCK$_{mt}$ does occur in tachyzoites (32), and genetic depletion of acetyl-CoA is associated with activation of gluconeogenesis (7). We therefore postulate that a decrease in the mitochondrial acetyl-CoA in the Δ*tggt1* mutant causes deacetylation of *Tg*PEPCK$_{mt}$, which turns on gluconeogenesis.

In conclusion, we show that the mitochondrial isoform of PEPCK embodies a main regulator linking catabolism of glucose and glutamine with anabolic routes in tachyzoites of *T. gondii*. Such a mechanism not only endows the parasite with the ability to concurrently assimilate two major carbon sources for biosynthetic activity but also sustains its survival when glucose becomes scarce. Hence, this work strengthens the notion that metabolic flexibility facilitating the utilization of multiple nutrients provides the parasite with a selective advantage to meet its bioenergetic demands in fluctuating nutritional milieus.

Materials and methods

Biological reagents and resources

Cell culture media and additives were purchased from Biochrom (Berlin, Germany). Other common chemicals were procured from AppliChem, Carl Roth, and Sigma-Aldrich. L-[U-^{13}C]glutamine was received from Euriso-top (Saarbrücken, Germany). Anti-HA and anti-biotin antibodies were acquired from Sigma-Aldrich. Fluorophore-conjugated antibodies (Alexa488/594) and oligonucleotides were obtained from Life Technologies (Ober-Olm, Germany). DNA-modifying enzymes were purchased from New England Biolabs (Frankfurt am Main, Germany). The RHΔ*ku80-hxgprt* (33, 34) and RHΔ*ku80*-TaTi (35) strains of *T. gondii* were provided by Vern Carruthers (University of Michigan) and Boris Striepen (University of Georgia), respectively. The RHΔ*ku80*-TaTi-Δ*tggt1* mutant was generated in our previous work (4). Primary antibodies against *Tg*F1B, *Tg*Fd (19), *Tg*Gap45 (36), and *Tg*Hsp90 (37) proteins were donated by Peter Bradley (University of California, Los Angeles, CA), Frank Seeber (Robert Koch Institute, Berlin), Dominique Soldati-Favre (University of Geneva, Switzerland), and Sergio Angel (National University of San Martín, Argentina), respectively.

Parasite culture and plaque assays

Tachyzoites of *T. gondii* (RHΔ*ku80-hxgprt*$^-$, RHΔ*ku80*-TaTi, and their derivative strains) were maintained by consecutive passage using human foreskin fibroblasts (HFFs) in a humidified incubator (37 °C, 5% CO_2). Cells were cultured in Dulbecco's modified Eagle's medium augmented with fetal calf serum (10%), glucose (4.5 g/liter), glutamine (2 mM), sodium pyruvate (1 mM), non-essential amino acids (100 μM serine, glycine, alanine, asparagine, aspartic acid, glutamate, and proline), penicillin (100 units/ml), and streptomycin (100 μg/ml). Parasites were cultured at an MOI of 3 on every second day. HFFs were harvested by trypsinization and grown to confluence in flasks/dishes. To isolate extracellular parasites, parasitized cultures (MOI = 3; 40–44-h infection) were washed with ice-cold PBS, scraped, and extruded through 23-gauge (1 time) and 27-gauge (2 times) syringes. Free tachyzoites were further purified from the remaining host cells by filtering (5 μm) and centrifugation (400 × *g*, 10 min, 4 °C). The viability of extracellular tachyzoites was examined by staining them with 0.6% fluorescein diacetate and ethidium bromide for 5 min, followed by fluorescence imaging (green, viable; red, dead). Our isolation procedure typically yielded viable parasites free of host cell debris.

The growth of individual parasite strains was measured by plaque assays in standard culture medium. Plaques recapitulate successive rounds of lytic cycles (*i.e.* invasion, replication, and egression) and therefore emulate the overall fitness of tachyzoites. Parasites were used to infect confluent HFF monolayers in 6-well plates (150 parasites/well) and incubated for 7 days. Cells were washed with PBS, fixed with methanol (−80 °C), and stained with crystal violet (15 min). Plaque images were analyzed using ImageJ software (National Institutes of Health, Bethesda, MD). About 100–200 plaques were scored for their area (arbitrary units) to evaluate the growth fitness of each parasite strain.

Ectopic and endogenous expression of epitope-tagged proteins in tachyzoites

The parasite RNA was isolated by a TRIzol-based extraction method and reverse-transcribed into first-strand cDNA using commercial kits (Life Technologies). For ectopic expression, the epitope-tagged ORFs of *Tg*PEPCK$_{mt}$ and *Tg*PyC were amplified from the tachyzoite-derived cDNA using PfuUltra II Fusion polymerase (Agilent Technologies) and matching primers (supplemental Table S1) followed by cloning into *pTETO7SAG1-UPKO* and *pTgGRA2-UPKO* plasmids. Both vectors allowed drug-selected insertion of the *Tg*PEPCK$_{mt}$ and *Tg*PyC expression cassettes at the *UPRT* locus using FUdR (38). The plasmid constructs (10 μg) were transfected into fresh extracellular tachyzoites (10^7) of the RHΔ*ku80-hxgprt*$^-$ or RHΔ*ku80*-TaTi-Δ*tggt1* strain by electroporation. Parasites were transformed in filter-sterile Cytomix (120 mM KCl, 0.15 mM $CaCl_2$, 10 mM K_2HPO_4/KH_2PO_4, 25 mM HEPES, 2 mM EGTA, 5 mM $MgCl_2$, 2 μM ATP, and 2 μM glutathione, pH 7.4) using a BTX instrument (2 kV, 50 ohms, 25 microfarads, 250 μs). Tachyzoites with a disrupted *UPRT* locus were selected by 5 μM FUdR (38).

The endogenous expression of *Tg*PyC, *Tg*PEPCK$_{mt}$, and *Tg*PEPCK$_{net}$ was determined by genomic tagging of the respective protein with an epitope in tachyzoites. To achieve this, a 1–1.5-kb-long crossover sequence (COS) targeting the 3′-end of the gene of interest was amplified from tachyzoite-derived gDNA and restriction-cloned into a plasmid for 3′-insertional tagging (*p3′IT-HXGPRT*) (see primers in supplemental Table S1). The constructs were linearized in the first half of the crossover sequence, as indicated in figures, and transfected into the RHΔ*ku80-hxgprt*$^-$ strain. Stable transgenic parasites expressing hypoxanthine-xanthine-guanine-phosphoribosyltransferase (HXGPRT) were selected using mycophenolic acid (25 μg/ml) and xanthine (50 μg/ml) (39). Genomic tagging was verified by recombination-specific PCR and sequencing. The eventual transgenic parasite strains harbored the epitope-tagged gene governed by native promoter and *Tg*GRA2-3′UTR.

Genetic deletions of TgPyC, TgPEPCK$_{mt}$, and TgPEPCK$_{net}$ in tachyzoites

The deletion of *TgPyC*, *TgPEPCK$_{mt}$*, and *TgPEPCK$_{net}$* genes was performed in the RHΔ*ku80*-TaTi (glycolysis-competent) and RHΔ*ku80*-TaTi-Δ*tggt1* (glycolysis-deficient) strains. A direct knock-out of the *TgPEPCK$_{mt}$* gene in the RHΔ*ku80*-TaTi-Δ*tggt1* strain was lethal; henceforth, we performed two-step conditional mutagenesis, which involved the making of an intermediate merodiploid strain expressing the ATc-regulatable ORF of *Tg*PEPCK$_{mt}$-HA governed by the *pTETO7SAG1* promoter, as described elsewhere (40). The knock-out constructs were generated by cloning 5′- and 3′-UTRs (1–2 kb) flanking a selection cassette encoding for pyrimethamine-resistant DHFR-TS in a plasmid for knock-out (*pKO-DHFR-TS*). 5′- and 3′-UTRs were amplified by genomic PCR using appropriate primers (supplemental Table S1). Parasites were selected with 1 μM pyrimethamine (41) and cloned by limiting dilution. The clonal mutants were identified by crossover-specific PCR screening of gDNA in conjunction with DNA sequencing.

Immunofluorescence and immunoblot assays

Confluent HFF cells grown on coverslips were infected with 4×10^5 tachyzoites for 24 h. Infected cultures were fixed with 4% paraformaldehyde (10 min). Samples were neutralized with 0.1% glycine/PBS for 5 min prior to permeabilization with 0.2% Triton X-100/PBS for 20 min. Cells were stained with specified primary antibodies (mouse/rabbit α-HA, 1:3000; mouse α-biotin, 1:10,000; rabbit α-*Tg*Gap45, 1:5000; rabbit α-*Tg*Hsp90, 1:10,000; rabbit α-*Tg*Fd, 1:500; mouse α-*Tg*F1B, 1:1000) and corresponding secondary antibodies (goat anti-mouse or anti-rabbit Alexa488/Alexa594, 1:10,000) for 1 h. Samples were mounted in Fluoromount G and DAPI, followed by image acquisition using an ApoTome microscope (Zeiss, Munich, Germany). For immunoblot analysis, protein samples isolated from fresh parasites (10^7) were resolved by 12% SDS-PAGE and transferred to a nitrocellulose membrane by semi-dry blotting. Blots were stained with designated primary (mouse α-HA, 1:3000; mouse α-biotin, 1:3000; rabbit α-*Tg*Hsp90, 1:3000) and secondary (IRDye® 680RD and IRDye® 800CW, 1:15,000) antibodies for 1 h. Protein bands were visualized using the LI-COR imaging system.

Stable isotope labeling and GC-MS measurement of central metabolites

Our primary objective was to demonstrate perturbation in transfer of glutamine-derived carbon to glycolysis and gluconeogenic metabolites in the ATc-repressible Δ*tggt1*/iΔ*tgpepck$_{mt}$* strain of *T. gondii*. HFFs were infected with control untreated and ATc-treated (60–72 h preculture in 1 μM ATc in standard culture medium) tachyzoites of the conditional mutant at MOI of 2.5 and 6, respectively, followed by incubation for 30 h in normal medium without or with the drug, as applicable. The regular medium was then replaced by isotope-containing medium with dialyzed FCS, in which normal glutamine was substituted by 5 mM [U-^{13}C]glutamine. Samples were incubated for the duration, as indicated in the respective figure legends. Cultures were quenched by ice cooling (5 min), and tachyzoites were isolated from host cells by syringe extrusion and filtering as stated above. Subsequently, parasites were washed with ice-cold PBS (400 × *g*, 10 min, 4 °C), counted, and subjected to metabolomic analyses.

Inclusion of [U-^{13}C]glutamine-derived carbon into polar metabolites was determined by gas chromatography and mass spectrometry. Metabolites of fresh extracellular parasites (1×10^8) were extracted in a mixture of chloroform, methanol, and water (1:3:1, v/v/v) for 20 min at 60 °C. Phase separation was induced by adding 200 μl of H_2O and 200 μl of chloroform. The polar phase was dried under vacuum and further processed, essentially as reported previously (4). In brief, the dry residue was derivatized with methoxyamine and *N*-methyl-*N*-(trimethylsilyl)-trifluoroacetamide solution in pyridine, and 3 μl of the derivatized mix was used for GC-MS. Metabolites were identified by their retention index and fragmentation patterns. Fractional abundance of ^{13}C atoms as well as of individual isotopomers is shown only for those metabolites that were reproducibly detectable in independent assays.

UPLC-MS measurement of ribose in nucleosides

Fresh parasites labeled with 5 mM [U-^{13}C]glutamine for 12 h, as described above, were counted, and 2×10^7 tachyzoites were processed for the RNA extraction using the innuPREP RNA minikit (Analytic Jena AG, Germany). Hydrolysis of the parasite RNA was performed using a method modified from Bratty *et al.* (42). Briefly, 5 μg of RNA was hydrolyzed in 250 μl of the digest mix containing 100 mM NaCl, 20 mM $MgCl_2$, 20 mM Tris (pH 7.9), 300 units of benzonase endonuclease (Sigma, E1014), 150 milliunits of phosphodiesterase I (Sigma, P3134), 25 units of alkaline phosphatase (Roche Diagnostics, 10713023001), 10 μg of *erythro*-9-(2-hydroxy-3-nonyl)-adenine hydrochloride (Sigma, E114), and 3 mM deferoxamine mesylate (Sigma, D9533). Hydrolysis was performed at 37 °C for 18 h. Hydrolyzed RNA was purified from enzymatic components using a Microcon centrifugal column filter unit (10-kDa cut-off, Millipore UK Ltd.; 3000 × *g*, 20 min).

RNA hydrolysates (~150 μl each) were 3× concentrated by drying in a vacuum centrifuge and then dissolving in 50 μl of water. The measurements were performed using a reversed phase UPLC device (Waters ACQUITY) coupled to a mass spectrometer (Thermo Fisher QExactive) (sample injection volume: 3 μl). Chromatographic conditions and operation of the electrospray were set, as reported by Giavalisco *et al.* (43). All measurements were performed in negative electrospray ionization mode, and each sample was measured twice. The first measurement was the DDA MS2 mode with Top3 ion selection and normalized collision energy set to 25 eV, followed by a total ion current scan. The DDA MS2 data were used to annotate individual nucleosides based on their fragmentation pattern by matching with the metaSysX reference library. Cytidine was not detectable in our assays, presumably due to non-enzymatic deamination into uridine during the preparation of samples. The total ion current data of the DDA MS2 analysis were used to estimate the inclusion of [U-^{13}C]glutamine into intact nucleosides. The second sample measurement was an inclusion list-based UPLC-MS/MS of all isotopomers of guanosine (as a purine representative) and uridine (a pyrimi-

dine representative) to establish the isotopomer profile of the ribose fragment (nominal m/z of 110 for non-labeled fragment and m/z from 111 to 115 for I+1 to I+5).

Calculation of the label inclusion in the GC-MS and UPLC-MS analysis

For the GC-MS data sets, the m/z peaks of non-fragmented or poorly fragmented metabolites were used to measure the isotope inclusion by calculating intensities of the unlabeled analyte and all labeled isotopomers. Intensities were corrected, taking into account both the natural enrichment for carbon and of silicon due to derivatization of samples producing TMS groups, as described in our previous work (4). For the UPLC-MS data sets, the data were corrected only for the natural abundance of ^{13}C isotope. The label inclusion into the ribose was calculated as intensity of non-labeled sugar isotopomer *versus* the intensity of all labeled isotopomers. It should be stated here that the fate of the isotope label does not reflect the immediate fate of labeled metabolites (44). The conditions tested in the present work are close to the equilibrium of label accumulation derived from [U-^{13}C]glutamine and from unlabeled glucose, pyruvate, and amino acids present in culture medium. Analysis of the individual isotopomer patterns as well as of concentrations of the precursors or of the final products would reflect the corresponding fluxes, which was not the aim of this study. However, in the case of a single passage point from TCA to glycolysis/gluconeogenesis pathway (as is the case for $PEPCK_{mt}$ in tachyzoites), changes in the total equilibrium labeling of pertinent metabolites, without regard to particular isotopomer pattern, do reflect the difference in the carbon transit between the two metabolic pathways under conditions of on- and off-states of the mitochondrial PEPCK enzyme.

Author contributions—R. N., Ö. G.-E., M. T., and V. Z. designed, performed, and analyzed experiments; N. G. conceived, designed, and coordinated the study and analyzed experiments; R. N. and N. G. wrote the paper. All authors reviewed and approved the manuscript.

Acknowledgments—We thank Grit Meusel (Humboldt University) for technical contributions to this work. We are grateful to Vern Carruthers (University of Michigan), Boris Striepen (University of Georgia), Dominique Soldati-Favre (University of Geneva, Switzerland), Sergio Angel (National University of San Martín, Argentina) Peter Bradley (University of California, Los Angeles, CA), and Frank Seeber (Robert Koch Institute, Berlin) for sharing biological reagents. Finally, we express our gratitude to the Toxoplasma database (www.ToxoDB.org) (45) community for enabling the gene identification and genome engineering work.

References

1. Blader, I. J., Coleman, B. I., Chen, C. T., and Gubbels, M. J. (2015) Lytic cycle of *Toxoplasma gondii*: 15 years later. *Annu. Rev. Microbiol.* **69,** 463–485
2. Blume, M., Rodriguez-Contreras, D., Landfear, S., Fleige, T., Soldati-Favre, D., Lucius, R., and Gupta, N. (2009) Host-derived glucose and its transporter in the obligate intracellular pathogen *Toxoplasma gondii* are dispensable by glutaminolysis. *Proc. Natl. Acad. Sci. U.S.A.* **106,** 12998–13003
3. MacRae, J. I., Sheiner, L., Nahid, A., Tonkin, C., Striepen, B., and McConville, M. J. (2012) Mitochondrial metabolism of glucose and glutamine is required for intracellular growth of *Toxoplasma gondii*. *Cell Host Microbe* **12,** 682–692
4. Nitzsche, R., Zagoriy, V., Lucius, R., and Gupta, N. (2016) Metabolic cooperation of glucose and glutamine is essential for the lytic cycle of obligate intracellular parasite *Toxoplasma gondii*. *J. Biol. Chem.* **291,** 126–141
5. Fleige, T., Fischer, K., Ferguson, D. J., Gross, U., and Bohne, W. (2007) Carbohydrate metabolism in the *Toxoplasma gondii* apicoplast: localization of three glycolytic isoenzymes, the single pyruvate dehydrogenase complex, and a plastid phosphate translocator. *Eukaryot. Cell* **6,** 984–996
6. Pomel, S., Luk, F. C. Y., and Beckers, C. J. M. (2008) Host cell egress and invasion induce marked relocations of glycolytic enzymes in *Toxoplasma gondii* tachyzoites. *PLoS Pathog.* **4,** e1000188
7. Oppenheim, R. D., Creek, D. J., Macrae, J. I., Modrzynska, K. K., Pino, P., Limenitakis, J., Polonais, V., Seeber, F., Barrett, M. P., Billker, O., McConville, M. J., and Soldati-Favre, D. (2014) BCKDH: the missing link in apicomplexan mitochondrial metabolism is required for full virulence of *Toxoplasma gondii* and *Plasmodium berghei*. *PLoS Pathog.* **10,** e1004263
8. Vander Heiden, M. G., Cantley, L. C., and Thompson, C. B. (2009) Understanding the Warburg effect: the metabolic requirements of cell proliferation. *Science* **324,** 1029–1033
9. DeBerardinis, R. J., Mancuso, A., Daikhin, E., Nissim, I., Yudkoff, M., Wehrli, S., and Thompson, C. B. (2007) Beyond aerobic glycolysis: transformed cells can engage in glutamine metabolism that exceeds the requirement for protein and nucleotide synthesis. *Proc. Natl. Acad. Sci. U.S.A.* **104,** 19345–19350
10. Berg, J. M., Tymoczko, J. L., and Stryer, L. (2002) Glucose can be synthesized from noncarbohydrate precursors. in *Biochemistry*, 5th Ed., Section 16.3, W.H. Freeman, New York
11. Cheng, T., Sudderth, J., Yang, C., Mullen, A. R., Jin, E. S., Matés, J. M., and DeBerardinis, R. J. (2011) Pyruvate carboxylase is required for glutamine-independent growth of tumor cells. *Proc. Natl. Acad. Sci. U.S.A.* **108,** 8674–8679
12. Montal, E. D., Dewi, R., Bhalla, K., Ou, L., Hwang, B. J., Ropell, A. E., Gordon, C., Liu, W. J., DeBerardinis, R. J., Sudderth, J., Twaddel, W., Boros, L. G., Shroyer, K. R., Duraisamy, S., Drapkin, R., *et al.* (2015) PEPCK coordinates the regulation of central carbon metabolism to promote cancer cell growth. *Mol. Cell* **60,** 571–583
13. Vincent, E. E., Sergushichev, A., Griss, T., Gingras, M. C., Samborska, B., Ntimbane, T., Coelho, P. P., Blagih, J., Raissi, T. C., Choinière, L., Bridon, G., Loginicheva, E., Flynn, B. R., Thomas, E. C., Tavaré, J. M., *et al.* (2015) Mitochondrial phosphoenolpyruvate carboxykinase regulates metabolic adaptation and enables glucose-independent tumor growth. *Mol. Cell* **60,** 195–207
14. Fleige, T., Pfaff, N., Gross, U., and Bohne, W. (2008) Localisation of gluconeogenesis and tricarboxylic acid (TCA)-cycle enzymes and first functional analysis of the TCA cycle in *Toxoplasma gondii*. *Int. J. Parasitol.* **38,** 1121–1132
15. Blume, M., Nitzsche, R., Sternberg, U., Gerlic, M., Masters, S. L., Gupta, N., and McConville, M. J. (2015) A *Toxoplasma gondii* gluconeogenic enzyme contributes to robust central carbon metabolism and is essential for replication and virulence. *Cell Host Microbe* **18,** 210–220
16. Jitrapakdee, S., St Maurice, M., Rayment, I., Cleland, W. W., Wallace, J. C., and Attwood, P. V. (2008) Structure, mechanism and regulation of pyruvate carboxylase. *Biochem. J.* **413,** 369–387
17. Hartmann, A., Hellmund, M., Lucius, R., Voelker, D. R., and Gupta, N. (2014) Phosphatidylethanolamine synthesis in the parasite mitochondrion is required for efficient growth but dispensable for survival of *Toxoplasma gondii*. *J. Biol. Chem.* **289,** 6809–6824
18. Jelenska, J., Crawford, M. J., Harb, O. S., Zuther, E., Haselkorn, R., Roos, D. S., and Gornicki, P. (2001) Subcellular localization of acetyl-CoA carboxylase in the apicomplexan parasite *Toxoplasma gondii*. *Proc. Natl. Acad. Sci. U.S.A.* **98,** 2723–2728
19. Vollmer, M., Thomsen, N., Wiek, S., and Seeber, F. (2001) Apicomplexan parasites possess distinct nuclear-encoded, but apicoplast-localized, plant-type ferredoxin-$NADP^+$ reductase and ferredoxin. *J. Biol. Chem.* **276,** 5483–5490
20. Hehl, A. B., Basso, W. U., Lippuner, C., Ramakrishnan, C., Okoniewski, M., Walker, R. A., Grigg, M. E., Smith, N. C., and Deplazes, P. (2015) Asexual

expansion of *Toxoplasma gondii* merozoites is distinct from tachyzoites and entails expression of non-overlapping gene families to attach, invade, and replicate within feline enterocytes. *BMC Genomics* **16,** 66

21. Des Rosiers, C., Di Donato, L., Comte, B., Laplante, A., Marcoux, C., David, F., Fernandez, C. A., and Brunengraber, H. (1995) Isotopomer analysis of citric acid cycle and gluconeogenesis in rat liver reversibility of isocitrate dehydrogenase and involvement of ATP-citrate lyase in gluconeogenesis. *J. Biol. Chem.* **270,** 10027–10036
22. Holleran, A. L., Briscoe, D. A., Fiskum, G., and Kelleher, J. K. (1995) Glutamine metabolism in AS-30D hepatoma cells: evidence for its conversion into lipids via reductive carboxylation. *Mol. Cell. Biochem.* **152,** 95–101
23. Chaudhary, K., Darling, J. A., Fohl, L. M., Sullivan, W. J., Jr., Donald, R. G., Pfefferkorn, E. R., Ullman, B., and Roos, D. S. (2004) Purine salvage pathways in the apicomplexan parasite *Toxoplasma gondii*. *J. Biol. Chem.* **279,** 31221–31227
24. Fox, B. A., and Bzik, D. J. (2002) *De novo* pyrimidine biosynthesis is required for virulence of *Toxoplasma gondii*. *Nature* **415,** 926–929
25. Lunt, S. Y., and Vander Heiden, M. G. (2011) Aerobic glycolysis: meeting the metabolic requirements of cell proliferation. *Annu. Rev. Cell Dev. Biol.* **27,** 441–464
26. Vacanti, N. M., Divakaruni, A. S., Green, C. R., Parker, S. J., Henry, R. R., Ciaraldi, T. P., Murphy, A. N., and Metallo, C. M. (2014) Regulation of substrate utilization by the mitochondrial pyruvate carrier. *Mol. Cell* **56,** 425–435
27. Limenitakis, J., Oppenheim, R. D., Creek, D. J., Foth, B. J., Barrett, M. P., and Soldati-Favre, D. (2013) The 2-methylcitrate cycle is implicated in the detoxification of propionate in *Toxoplasma gondii*. *Mol. Microbiol.* **87,** 894–908
28. Stein, W. H., and Moore, S. (1954) The free amino acids of human blood plasma. *J. Biol. Chem.* **211,** 915–926
29. Méndez-Lucas, A., Hyroššová, P., Novellasdemunt, L., Viñals, F., and Perales, J. C. (2014) Mitochondrial phosphoenolpyruvate carboxykinase (PEPCK-M) is a pro-survival, endoplasmic reticulum (ER) stress response gene involved in tumor cell adaptation to nutrient availability. *J. Biol. Chem.* **289,** 22090–22102
30. Stark, R., Pasquel, F., Turcu, A., Pongratz, R. L., Roden, M., Cline, G. W., Shulman, G. I., and Kibbey, R. G. (2009) Phosphoenolpyruvate cycling via mitochondrial phosphoenolpyruvate carboxykinase links anaplerosis and mitochondrial GTP with insulin secretion. *J. Biol. Chem.* **284,** 26578–26590
31. Jiang, W., Wang, S., Xiao, M., Lin, Y., Zhou, L., Lei, Q., Xiong, Y., Guan, K. L., and Zhao, S. (2011) Acetylation regulates gluconeogenesis by promoting PEPCK1 degradation via recruiting the UBR5 ubiquitin ligase. *Mol. Cell* **43,** 33–44
32. Jeffers, V., and Sullivan, W. J., Jr. (2012) Lysine acetylation is widespread on proteins of diverse function and localization in the protozoan parasite *Toxoplasma gondii*. *Eukaryot. Cell* **11,** 735–742
33. Fox, B. A., Ristuccia, J. G., Gigley, J. P., and Bzik, D. J. (2009) Efficient gene replacements in *Toxoplasma gondii* strains deficient for nonhomologous end joining. *Eukaryot. Cell* **8,** 520–529
34. Huynh, M. H., and Carruthers, V. B. (2009) Tagging of endogenous genes in a *Toxoplasma gondii* strain lacking Ku80. *Eukaryot. Cell* **8,** 530–539
35. Sheiner, L., Demerly, J. L., Poulsen, N., Beatty, W. L., Lucas, O., Behnke, M. S., White, M. W., and Striepen, B. (2011) A systematic screen to discover and analyze apicoplast proteins identifies a conserved and essential protein import factor. *PLoS Pathog.* **7,** e1002392
36. Plattner, F., Yarovinsky, F., Romero, S., Didry, D., Carlier, M. F., Sher, A., and Soldati-Favre, D. (2008) *Toxoplasma* profilin is essential for host cell invasion and TLR11-dependent induction of an interleukin-12 response. *Cell Host Microbe* **3,** 77–87
37. Echeverria, P. C., Figueras, M. J., Vogler, M., Kriehuber, T., de Miguel, N., Deng, B., Dalmasso, M. C., Matthews, D. E., Matrajt, M., Haslbeck, M., Buchner, J., and Angel, S. O. (2010) The Hsp90 co-chaperone p23 of *Toxoplasma gondii*: identification, functional analysis and dynamic interactome determination. *Mol. Biochem. Parasitol.* **172,** 129–140
38. Donald, R. G., and Roos, D. S. (1995) Insertional mutagenesis and marker rescue in a protozoan parasite: cloning of the uracil phosphoribosyltransferase locus from *Toxoplasma gondii*. *Proc. Natl. Acad. Sci. U.S.A.* **92,** 5749–5753
39. Donald, R. G., Carter, D., Ullman, B., and Roos, D. S. (1996) Insertional tagging, cloning, and expression of the *Toxoplasma gondii* hypoxanthine-xanthine-guanine phosphoribosyltransferase gene: use as a selectable marker for stable transformation. *J. Biol. Chem.* **271,** 14010–14019
40. Meissner, M., Schlüter, D., and Soldati, D. (2002) Role of *Toxoplasma gondii* myosin A in powering parasite gliding and host cell invasion. *Science* **298,** 837–840
41. Donald, R. G., and Roos, D. S. (1993) Stable molecular transformation of *Toxoplasma gondii*: a selectable dihydrofolate reductase-thymidylate synthase marker based on drug-resistance mutations in malaria. *Proc. Natl. Acad. Sci. U.S.A.* **90,** 11703–11707
42. Bratty, M. A., Chintapalli, V. R., Dow, J. A., Zhang, T., and Watson, D. G. (2012) Metabolomic profiling reveals that *Drosophila melanogaster* larvae with the y mutation have altered lysine metabolism. *FEBS Open Bio* **2,** 217–221
43. Giavalisco, P., Köhl, K., Hummel, J., Seiwert, B., and Willmitzer, L. (2009) ^{13}C isotope-labeled metabolomes allowing for improved compound annotation and relative quantification in liquid chromatography-mass spectrometry-based metabolomic research. *Anal. Chem.* **81,** 6546–6551
44. Krebs, H. A., Hems, R., Weidemann, M. J., and Speake, R. N. (1966) The fate of isotopic carbon in kidney cortex synthesizing glucose from lactate. *Biochem. J.* **101,** 242–249
45. Gajria, B., Bahl, A., Brestelli, J., Dommer, J., Fischer, S., Gao, X., Heiges, M., Iodice, J., Kissinger, J. C., Mackey, A. J., Pinney, D. F., Roos, D. S., Stoeckert, C. J., Jr., Wang, H., and Brunk, B. P. (2008) ToxoDB: an integrated *Toxoplasma gondii* database resource. *Nucleic Acids Res.* **36,** D553–D556